

# DISCRETE QUASI-EIGENFUNCTION APPROXIMATION FOR AM-FM IMAGE ANALYSIS

Joseph P. Havlicek, David S. Harding, and Alan C. Bovik

Laboratory for Vision Systems, University of Texas, Austin, TX 78712-1084

## ABSTRACT

We introduce a multidimensional quasi-eigenfunction approximation useful for characterizing and analyzing the responses of discrete linear systems to inputs modeled as AM-FM image functions. A new theorem is presented which provides a global bound on the approximation error. We demonstrate how the approximation may be used to develop discrete AM-FM demodulation algorithms, and show dramatic demodulation examples where the essential structure of natural images is captured using only a small number of AM-FM components.

## 1. INTRODUCTION

The use of AM-FM modeling techniques for analysis and representation of nonstationary signals and images has been the subject of intense recent research [1-8]. In multi-component AM-FM image analysis, a complex-valued image  $t(\mathbf{x})$  is modeled as a sum of nonstationary, locally coherent AM-FM functions

$$t(\mathbf{x}) = \sum_{k=1}^K a_k(\mathbf{x}) \exp[j\varphi_k(\mathbf{x})], \quad (1)$$

where  $\mathbf{x} = [x_1, x_2]^T$ ,  $t: \mathbb{R}^2 \rightarrow \mathbb{C}$ ,  $a_k: \mathbb{R}^2 \rightarrow [0, \infty)$ , and  $\varphi_k: \mathbb{R}^2 \rightarrow \mathbb{R}$ . A real-valued image  $s(\mathbf{x})$  may be analyzed against the model (1) using the unique complex extension  $t(\mathbf{x}) = s(\mathbf{x}) + j\mathcal{H}[s(\mathbf{x})]$ , where  $\mathcal{H}[\cdot]$  indicates the 2D Hilbert transform acting in the horizontal direction. The AM-FM analysis problem is concerned with estimating the amplitude modulation functions  $a_k(\mathbf{x})$  and the frequency modulation functions  $\nabla\varphi_k(\mathbf{x})$ . This is normally accomplished using nonlinear algorithms, making it necessary to isolate the individual components from one another prior to performing the estimation in order to avoid cross-component interference effects. The separation may be effected on a spatio-spectrally localized basis by processing the image with a multiband linear filter bank.

However, the development of frequency demodulation algorithms for filtered components is, in general, quite difficult. Excellent approximate estimation algorithms have been derived by making use of a family of approximations known collectively as *quasi-eigenfunction approximations*,

This research was supported in part by a grant from the Texas Advanced Research Projects Agency and by the Air Force Office of Scientific Research, Air Force Systems Command, USAF, under grant number F49620-93-1-0307.

or *QEAs* [3, 5, 6, 9-12]. The exact response of the filter  $g(\mathbf{x})$  to image component  $t_k(\mathbf{x}) = a_k(\mathbf{x}) \exp[j\varphi_k(\mathbf{x})]$  is

$$d(\mathbf{x}) = \int_{\mathbb{R}^2} t_k(\mathbf{x} - \mathbf{y})g(\mathbf{y})d\mathbf{y}. \quad (2)$$

The QEA for the response is

$$\hat{d}(\mathbf{x}) = t_k(\mathbf{x})G[\nabla\varphi_k(\mathbf{x})], \quad (3)$$

where  $G(\Omega) = \mathcal{F}[g(\mathbf{x})]$  is the Fourier transform of  $g(\mathbf{x})$ . Note that *all* quantities in the QEA (3) are spatially varying. The approximation is exact if  $t_k(\mathbf{x})$  is *monochromatic*, *viz.* if the modulating functions are both constant. Otherwise there is generally an error in (3). However, theoretical results tightly bounding the approximation error have been obtained for the case of 1D continuous-domain signals [9], 1D discrete-domain signals [6, 11, 12], and multi-dimensional continuous-domain signals [5, 10]. The errors are generally small, provided that the filter impulse response is localized and the modulating functions are smooth, or *locally coherent*. The 2D continuous-domain QEA may be used to establish the validity of the following approximate, filtered AM-FM demodulation algorithm:

$$\nabla\varphi_k(\mathbf{x}) \approx \nabla\hat{\varphi}_k(\mathbf{x}) = \text{Re} \left[ \frac{\nabla d(\mathbf{x})}{jd(\mathbf{x})} \right], \quad (4)$$

$$a_k(\mathbf{x}) \approx \hat{a}_k(\mathbf{x}) = \left| \frac{d(\mathbf{x})}{G[\nabla\hat{\varphi}_k(\mathbf{x})]} \right|. \quad (5)$$

Since the algorithm (4), (5) is spatially local, it is only necessary for the filtering operation described in (2) to separate the components from one another on a *pointwise* basis; the filter response may, in general, be dominated by different image components at different points in the domain. The demodulation algorithm is valid for the dominating component, provided that at most one component dominates the response image at each point.

In this paper we present, for the first time, the discrete 2D QEA and a bound on the approximation error. We use the approximation to develop discrete-domain AM-FM demodulation algorithms. This is significant since images almost *always* are acquired as discrete-domain signals, since there are considerable differences between the 1D and 2D discrete bounds, and since there are subtleties in discretizing the algorithm (4), (5).

## 2. THE 2D DISCRETE QEA

We approximate the response of absolutely summable, 2D discrete linear systems to AM-FM inputs and bound the

approximation error. Consider a discrete, complex-valued AM-FM image component

$$c(\mathbf{m}) = a(\mathbf{m}) \exp[j\varphi(\mathbf{m})] \quad (6)$$

and an arbitrary discrete linear system  $g : \mathbb{Z}^2 \rightarrow \mathbb{C}$  with unit pulse response  $g(\mathbf{m}) \in \ell^1(\mathbb{Z}^2)$  and frequency response  $G(\Omega)$ . Henceforth, we write  $g(\mathbf{m}) \Leftrightarrow G(\Omega)$  to indicate that  $g(\mathbf{m})$  and  $G(\Omega)$  are a Fourier transform pair. The exact response of  $G$  to input  $c(\mathbf{m})$  is given by

$$d(\mathbf{m}) = \sum_{\mathbf{p} \in \mathbb{Z}^2} g(\mathbf{p}) c(\mathbf{m} - \mathbf{p}). \quad (7)$$

The quasi-eigenfunction approximation to the response is

$$\hat{d}(\mathbf{m}) = c(\mathbf{m}) G[\nabla\varphi(\mathbf{m})], \quad (8)$$

where  $\nabla\varphi(\mathbf{m}) = \nabla\varphi(\mathbf{x})|_{\mathbf{x}=\mathbf{m}}$ . Note that the form of the QEA in (8) is analogous to the eigenfunction interpretation of the response of a discrete linear system to a monochromatic input. While an arbitrary image component modeled as an AM-FM function may bear little similarity to an eigenfunction of  $g(\mathbf{m})$  when viewed at a *global* scale, all of the quantities involved in the approximation (8) are *spatially localized*. If the modulating functions of  $c(\mathbf{m})$  are locally coherent at scales smaller than the spatial support of  $g(\mathbf{m})$ , then we reason that  $c(\mathbf{m})$  may look very much like an eigenfunction on a spatially local basis. In the theorem below, we provide a global bound on the approximation error. First, we introduce some convenient notation.

Let  $\varepsilon_d(\mathbf{m})$  denote the error in the 2D QEA:  $\varepsilon_d(\mathbf{m}) = |d(\mathbf{m}) - \hat{d}(\mathbf{m})|$ . Denote the maximum value of the amplitude modulation function  $a(\mathbf{m})$  by  $a_{\max} = \max_{\mathbf{p}} a(\mathbf{p})$ , and the absolute sum of a sequence by  $\|g\|_{\ell^1} = \sum_{\mathbf{p} \in \mathbb{Z}^2} |g(\mathbf{p})|$ .

Use the notation  $\mathcal{L}_n(\mathbf{F})$  to denote the supremum of the magnitudes of all line integrals of the vector-valued function  $\mathbf{F}$  along paths  $\sigma(s) \in P^n$ , where  $P^n$  is the space of polynomials with degree less than or equal to  $n$ . Thus

$$\mathcal{L}_n(\mathbf{F}) = \sup_{\sigma \in P^n} \left| \int_{\sigma} \mathbf{F}(\mathbf{x}) \cdot d\mathbf{x} \right|. \quad (9)$$

Similarly, use the notation  $\mathcal{G}_n(\mathbf{F})$  to denote the supremum of all line integrals of the *magnitude* of the vector-valued function  $\mathbf{F}$  along paths  $\sigma(s) \in P^n$ :

$$\mathcal{G}_n(\mathbf{F}) = \sup_{\sigma \in P^n} \int_{\sigma} |\mathbf{F}(\mathbf{x})| ds. \quad (10)$$

Let  $\mathbf{e}_i$  denote the unit vector in the  $i$  direction:  $\mathbf{e}_1 = [1, 0]^T$ ,  $\mathbf{e}_2 = [0, 1]^T$ . Let  $\varphi_{x_i}(\mathbf{x}) = \frac{\partial}{\partial x_i} \varphi(\mathbf{x})$ , the partial of  $\varphi(\mathbf{x})$  in the  $\mathbf{e}_i$  direction. Finally, quantify the spatial duration of the filter  $g(\mathbf{m})$  in the  $\mathbf{e}_i$  direction using the generalized moment functional

$$\Delta_i(g) = \sum_{\mathbf{p} \in \mathbb{Z}^2} |\mathbf{p} \mathbf{e}_i^T \mathbf{p}| |g(\mathbf{p})|. \quad (11)$$

**Theorem:** Let  $c(\mathbf{m})$  be as in (6) and let  $a(\mathbf{m})$ ,  $\varphi(\mathbf{m})$ , and  $g(\mathbf{m}) \in \ell^1(\mathbb{Z}^2)$ . Let  $a(\mathbf{x})$  be continuously partially differentiable and  $\varphi(\mathbf{x})$  be twice continuously partially differentiable. Let  $\varepsilon_d(\mathbf{m})$  be as defined above. Then

$$\varepsilon_d(\mathbf{m}) \leq \{ \|g\|_{\ell^1} - |g(0)| \} \mathcal{L}_1(\nabla a) + a_{\max} \{ \Delta_1(g) \mathcal{G}_1(\nabla\varphi_{x_1}) + \Delta_2(g) \mathcal{G}_1(\nabla\varphi_{x_2}) \} \quad (12)$$

**Proof:** omitted for brevity.

The error bound in (12) is global in the sense that it is independent of the spatial coordinates. Note that the term  $\mathcal{L}_1(\nabla a)$ , the supremum of the magnitudes of all line integrals of  $\nabla a(\mathbf{x})$  along straight paths, tends to grow inversely with the smoothness of  $a(\mathbf{x})$ , and vanishes altogether in the limit as  $c(\mathbf{m})$  tends toward a true eigenfunction. The terms  $\mathcal{G}_1(\nabla\varphi_{x_1})$  and  $\mathcal{G}_1(\nabla\varphi_{x_2})$ , which are the suprema of all line integrals of the gradient magnitudes of the components of the instantaneous frequency vector along straight paths, also tend to grow inversely with the smoothness of  $\varphi(\mathbf{x})$ , and vanish as  $c(\mathbf{m})$  tends to a true eigenfunction. Hence, the QEA errors will be small when the input is locally coherent. Furthermore, the bound in (12) is tight in the sense that it tends to zero as  $c(\mathbf{m})$  tends to an eigenfunction of  $g(\mathbf{m})$ . Also of interest is the fact that both terms in the bound (12) can be made arbitrarily small through the choice of a filter  $g(\mathbf{m})$  that is highly spatially localized. This is true independent of the local coherency of the input  $c(\mathbf{m})$ .

### 3. APPLICATION TO AM-FM IMAGE DEMODULATION

We begin by using the QEA to develop demodulation algorithms for an *unfiltered* image component. Consider a system parameterized by constants  $n_1, n_2 \in \mathbb{Z}$  and  $q = \pm 1$ , where the unit pulse response and frequency response of the system are

$$\begin{aligned} h_i(\mathbf{m}) &= \delta(\mathbf{m} + n_1 \mathbf{e}_i) + q\delta(\mathbf{m} + n_2 \mathbf{e}_i) \\ &\Leftrightarrow H_i(\Omega) = e^{jn_1 \Omega^T \mathbf{e}_i} + qe^{jn_2 \Omega^T \mathbf{e}_i}. \end{aligned} \quad (13)$$

The exact response of  $h_i$  to the component (6) is

$$s(\mathbf{m}) = c(\mathbf{m}) * h_i(\mathbf{m}) = c(\mathbf{m} + n_1 \mathbf{e}_i) + qc(\mathbf{m} + n_2 \mathbf{e}_i), \quad (14)$$

while the QEA is

$$\begin{aligned} \hat{s}(\mathbf{m}) &= c(\mathbf{m}) \{ \exp[jn_1 \mathbf{e}_i^T \nabla\varphi(\mathbf{m})] \\ &\quad + q \exp[jn_2 \mathbf{e}_i^T \nabla\varphi(\mathbf{m})] \}. \end{aligned} \quad (15)$$

Equating (14) and (15) with  $n_1 = 1$  and  $n_2 = q = -1$ , we have almost immediately that

$$\begin{aligned} \mathbf{e}_i^T \nabla\varphi(\mathbf{m}) &\approx \mathbf{e}_i^T \nabla\hat{\varphi}(\mathbf{m}) \\ &= \arcsin \left[ \frac{c(\mathbf{m} + \mathbf{e}_i) - c(\mathbf{m} - \mathbf{e}_i)}{2jc(\mathbf{m})} \right], \end{aligned} \quad (16)$$

while choosing  $n_1 = q = 1$  and  $n_2 = -1$  yields

$$\begin{aligned} \mathbf{e}_i^T \nabla\varphi(\mathbf{m}) &\approx \mathbf{e}_i^T \nabla\hat{\varphi}(\mathbf{m}) \\ &= \arccos \left[ \frac{c(\mathbf{m} + \mathbf{e}_i) + c(\mathbf{m} - \mathbf{e}_i)}{2c(\mathbf{m})} \right]. \end{aligned} \quad (17)$$

The algorithms (16), (17), called the *Sine* and *Cosine* algorithms respectively, are the discrete equivalents of (4). They may be used individually to estimate the components of the frequency modulation vector to within  $\pi$  radians, or together to place the frequencies to within  $2\pi$  radians. The amplitude modulation  $a(\mathbf{m})$  is estimated by  $\hat{a}(\mathbf{m}) = |c(\mathbf{m})|$ .

Next, we use the QEA to develop algorithms for estimating the modulating functions of  $c(\mathbf{m})$  in (6) from the filtered component  $d(\mathbf{m})$  given by (7). Consider a cascade system  $f(\mathbf{m}) = g(\mathbf{m}) * h_i(\mathbf{m})$ , where  $g(\mathbf{m}) \in \ell^1(\mathbb{Z}^2)$  as before, and  $h_i$  is as defined in (13). By definition, the response of the cascade system to input (6) is

$$r(\mathbf{m}) = c(\mathbf{m}) * f(\mathbf{m}) \quad (18)$$

$$= d(\mathbf{m}) * h_i(\mathbf{m}). \quad (19)$$

Using (13), Equation (19) may be expressed as

$$r(\mathbf{m}) = d(\mathbf{m} + n_1 \mathbf{e}_i) + qd(\mathbf{m} + n_2 \mathbf{e}_i). \quad (20)$$

Applying the QEA first to (18), and then to (7), we have

$$\hat{r}(\mathbf{m}) = c(\mathbf{m})G[\nabla\varphi(\mathbf{m})] \left\{ \exp[jn_1 \mathbf{e}_i^T \nabla\varphi(\mathbf{m})] + q \exp[jn_2 \mathbf{e}_i^T \nabla\varphi(\mathbf{m})] \right\} \quad (21)$$

$$= \hat{d}(\mathbf{m}) \left\{ \exp[jn_1 \mathbf{e}_i^T \nabla\varphi(\mathbf{m})] + q \exp[jn_2 \mathbf{e}_i^T \nabla\varphi(\mathbf{m})] \right\}. \quad (22)$$

Equating (20) with (22), subject to the QEA error, establishes immediately that both the Sine and Cosine algorithms may be applied directly to the filtered image  $d(\mathbf{m})$  in (7) to obtain  $\nabla\hat{\varphi}(\mathbf{m})$ . In estimating the amplitude modulation of  $c(\mathbf{m})$  from  $d(\mathbf{m})$ , the scaling effects of the filter  $g(\mathbf{m})$  must be factored out. Hence, it follows from the QEA that the discrete, filtered amplitude algorithm is

$$a(\mathbf{m}) \approx \hat{a}(\mathbf{m}) = \left| \frac{d(\mathbf{m})}{G[\nabla\hat{\varphi}(\mathbf{m})]} \right|. \quad (23)$$

#### 4. EXAMPLES

In this section we present dramatic new examples of multi-component AM-FM image analysis and representation. In each example, components were isolated from one another using a spatio-spectrally localized multiband bank of one-octave Gabor filters in a wavelet-like tessellation [10]. The modulating functions of individual components were then estimated from the channel responses using the discrete demodulation algorithms (16), (17), and (23).

An analysis paradigm called *dominant component analysis*, or *DCA*, was described in [5]. The object of DCA is to estimate, at each point in the image, the values of the modulating functions of the component that dominates the local image spectrum at that point. The frequencies so obtained are termed *emergent*, and characterize the dominant features of the local texture structure. Fig. 1 (a) shows the image *Tree*. The estimated emergent frequencies are shown in Fig. 1 (b), where each needle is oriented with the estimated frequency vector and needle length is inversely proportional to the frequency magnitude. Hence, long needles correspond to *low* spatial frequencies and image features of large spatial extent, while short needles correspond to *high* spatial frequencies and image features of small spatial extent. A reconstruction of the *dominant* component of the image from the estimated frequency and amplitude modulation functions (the latter is not depicted) is given in Fig. 1 (c). While the AM-FM component obtained from

DCA is not necessarily locally coherent, it reveals the *dominant* structure of the image on a spatially local basis using only a *single* AM-FM component.

The details of an approach for simultaneously estimating the modulating functions of multiple AM-FM image components from the Gabor channel responses was also described in [5]. The image *Reptile* is shown in Fig. 1 (d). Modulating functions for five nonstationary, locally coherent AM-FM components of this image were estimated using (16), (17), and (23). Reconstructions of the individual components from the estimated modulating functions are shown in Fig. 1 (e) - (g), (i), and (j). The effects of smooth, nonstationary variations in both the amplitude and frequency modulating functions are clearly visible. Fig. 1 (h) shows the reconstructed image obtained from the estimated modulating functions of all five components. It is truly remarkable that the essential structure of the image has been effectively captured with such a small number of components.

Similarly, Fig. 1 (k) and (l) show the image *Burlap* and a reconstruction from the estimated modulating functions of eight nonstationary, locally coherent AM-FM components. Again, this example clearly demonstrates the power of AM-FM modeling to capture the essential and perceptually important structure in a complicated image using only a small number of nonstationary, locally coherent AM-FM components.

#### 5. CONCLUSIONS

For the first time, we gave a *discrete* multidimensional quasi-eigenfunction approximation for analyzing the responses of discrete linear systems to AM-FM inputs. We also gave a new theorem bounding the approximation error. Using the approximation, we established discrete algorithms suitable for simultaneously estimating the modulating functions of multiple image components from the responses of linear multiband filters. The filters were required to separate the components from one another on a spatio-spectrally localized basis. We used the discrete demodulation algorithms to estimate modulating functions for the multiple components of three natural images, and demonstrated the power of AM-FM modeling techniques to capture and represent the essential structure of images using fewer than ten components.

#### 6. REFERENCES

- [1] P. Maragos and A. C. Bovik, "Image demodulation using multidimensional energy separation", *J. Opt. Soc. Amer. A*, vol. 12, no. 9, pp. 1867-1876, September 1995.
- [2] P. Maragos, J. F. Kaiser, and T. F. Quatieri, "Energy separation in signal modulations with applications to speech analysis", *IEEE. Trans. Signal Proc.*, vol. SP-41, no. 10, pp. 3024-3051, October 1993.
- [3] J. P. Havlicek, D. S. Harding, and A. C. Bovik, "Reconstruction from the multi-component AM-FM image representation", in *Proc. IEEE Int'l. Conf. Image Proc.*, Washington, DC, October 22-25 1995, pp. II280 - II283.

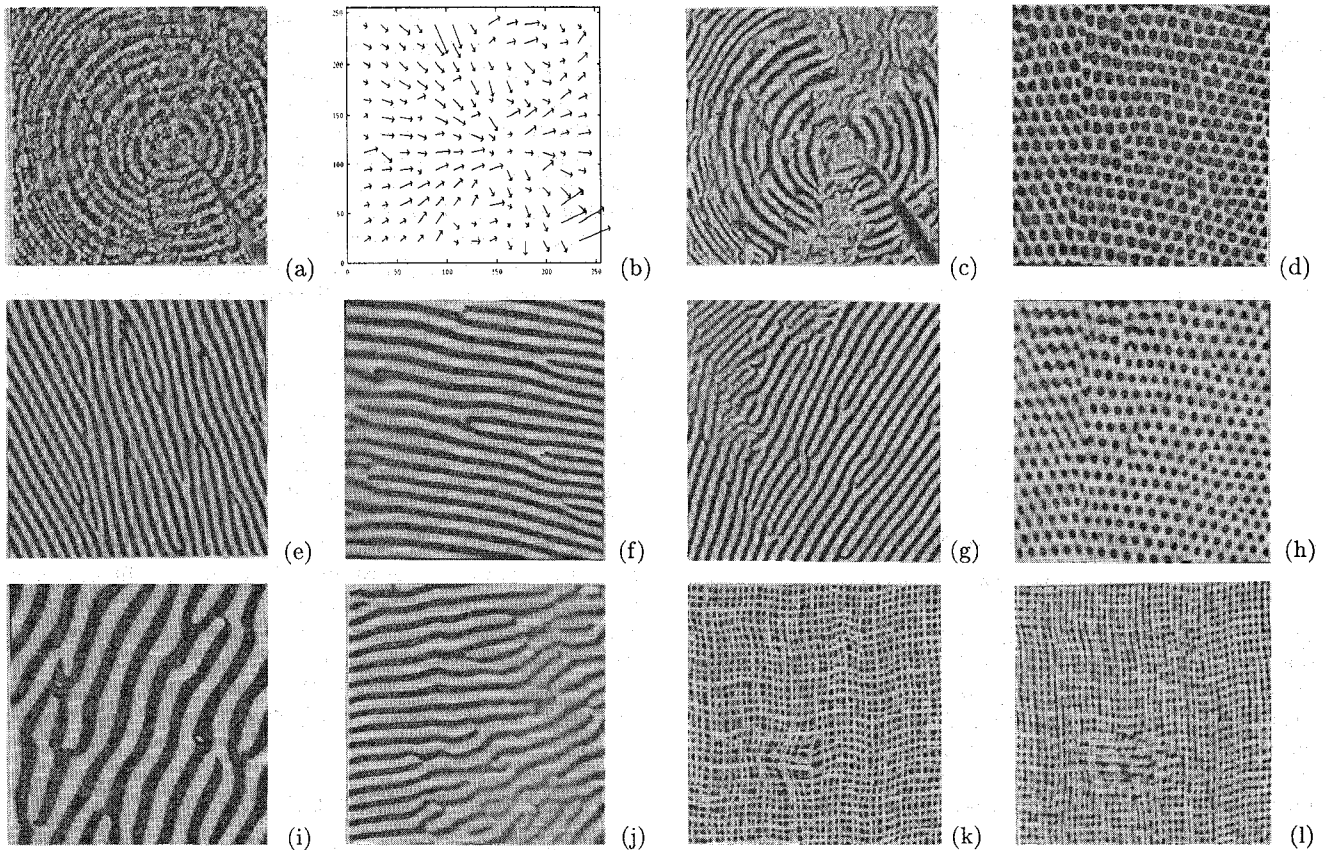


Figure 1: AM-FM discrete demodulation examples. (a) Tree image. (b) Estimated frequency modulation for Tree dominant component. Needle length is proportional to instantaneous period. (c) Reconstruction of Tree dominant component from estimated modulating functions. (d) Reptile image. (e)-(g) Three AM-FM image components of Reptile, reconstructed from estimated modulating functions. (h) Reconstruction of essential structure of Reptile from estimated modulating functions of five AM-FM components, as shown in (e)-(g),(i),(j). (i)-(j) Remaining two reconstructed components of Reptile. (k) Burlap image. (l) Reconstruction of Burlap from estimated modulating functions of eight AM-FM components.

- [4] P. Maragos and A. C. Bovik, "Demodulation of images modeled by amplitude-frequency modulation using multidimensional energy separation", in *Proc. IEEE Int'l. Conf. Image Proc.*, Austin, TX, 1994, pp. III421-III425.
- [5] J. P. Havlicek, D. S. Harding, and A. C. Bovik, "The mutli-component AM-FM image representation", *IEEE Trans. Image Proc.*, June 1996.
- [6] A. C. Bovik, J. P. Havlicek, D. S. Harding, and M. D. Desai, "Limits on discrete modulated signals", *IEEE Trans. Signal Proc.*, submitted.
- [7] S. Lu and P. C. Doerschuk, "Nonlinear modeling and processing of speech based on sums of AM-FM formant models", *IEEE. Trans. Signal Proc.*, vol. SP-44, no. 4, pp. 773-782, April 1996.
- [8] D. Vakman, "On the analytic signal, the Teager-Kaiser energy algorithm, and other methods for defining amplitude and frequency", *IEEE. Trans. Signal Proc.*, vol. SP-44, no. 4, pp. 791-797, April 1996.
- [9] A. C. Bovik, P. Maragos, and T. F. Quatieri, "AM-FM energy detection and separation in noise using multi-band energy operators", *IEEE. Trans. Signal Proc.*, vol. SP-41, no. 12, pp. 3245-3265, December 1993.
- [10] A. C. Bovik, N. Gopal, T. Emmoth, and A. Restrepo, "Localized measurement of emergent image frequencies by Gabor wavelets", *IEEE. Trans. Info. Theory*, vol. IT-38, no. 2, pp. 691-712, March 1992.
- [11] A. C. Bovik, J. P. Havlicek, and M. D. Desai, "Theorems for discrete filtered modulated signals", in *Proc. IEEE Int'l. Conf. Acoust., Speech, Signal Proc.*, Minneapolis, MN, April 27 - 30 1993, pp. III153-III156.
- [12] J. P. Havlicek, A. C. Bovik, M. D. Desai, and D. S. Harding, "The discrete quasi-eigenfunction approximation", in *Proc. Int'l. Conf. on Digital Signal Proc.*, Limassol, Cyprus, June 26 - 28 1995.